Indian Geotechnical Journal, 29 (3), 1999

Analysis of Pile Groups Subjected to Cyclic Lateral Loading

V.A. Sawant† and D.M. Dewaikar‡

Introduction

Pile group foundations involve three-dimensional interaction between pile-cap, soil and piles. In the past, the problem has often been solved by making assumptions regarding geometry and material properties. However, to account for the realistic nature of the problem, it is necessary to allow for three-dimensional geometry, interface effects and non-linear soil properties. Cyclic lateral loading is an aspect of the problem that introduces additional complexity and is encountered in offshore foundations as well as other applications. Structures like offshore platforms are subjected to cyclic loading due to wave action. The limited information available on the effects of cyclic loading on piles indicates that remarkable reduction in load capacity and pile-soil system stiffness can occur. In some of these cases, failure is characterised by a continued accumulation of permanent displacements resulting in movements of pile of the order of one pile diameter after several cycles of load application. It appears that at least two mechanisms may contribute to the failure of piles under cyclic loading :

1. Cyclic degradation of soil modulus and yield stress; this may be expected to dominate under essentially two-way cyclic loading.

2. Accumulation of permanent displacement with increasing load cycles; this may be expected to dominate under essentially one-way cyclic loading.

---

† Research Scholar, Civil Engineering Department, Indian Institute of Technology, Powai, Mumbai – 400076, India.

‡ Professor, Civil Engineering Department, Indian Institute of Technology, Powai, Mumbai – 400076, India.

The purpose of this paper is to present an iterative three-dimensional finite element procedure, which incorporates effects of cyclic loading and material nonlinearity. Material nonlinearity of the soil medium is represented by a bilinear model, in which, yield surface is defined by von-Mises yield criterion. The non-linear behaviour of interface is also modelled by bilinear relationship between interface shear stress and relative shear displacement. A parametric study is conducted to investigate the behaviour of a single pile and pile groups, embedded in homogeneous clay, with different pile spacings and arrangement of piles in group, subjected to one-way and two-way cyclic lateral loading.

Brief Review

A matrix approach for obtaining individual pile forces in a pile group was first proposed by Hrennikoff (1949), who solved the problem using a two-dimensional idealisation. Although this method of analysis has considerable generality in solving the pile group problems, the surrounding soil is approximated as a linear Winkler medium. Also, this method of analysis is usually valid if the cap is highly rigid. Reese and O'Neill (1970), extended Hrennikoff's method of analysis to a three-dimensional batter pile foundation. The torsional degree of freedom is also considered in their analysis. The axial, lateral and torsional behaviours are assumed to be linearly independent, and the total pile head reactions are obtained by superposition. This method also used Winkler soil model.

Banerjee and Driscoll (1976), used the boundary element method for the analysis of vertical pile groups. They assumed linear elastic behaviour for soil, and no relative movements between the soil and piles were allowed. Kim and Brungraber (1976), carried out full scale lateral load tests on vertical and batter pile groups arranged in different configurations. The results indicated that, with increase in spacing, there was an increase in the resistance to lateral loads. The procedure proposed by Desai et al. (1981) uses beam-column, plate and non-linear spring elements for simulating piles, cap and foundations, respectively. One of the limitations of this type of analysis is that pile cap should be fairly thin, so that it can be treated as a thin plate.

Muqtadir and Desai (1986) presented a non-linear three-dimensional finite element procedure for the analysis of a pile group. Zaman et al., (1993) studied the effects of pile-cap thickness and pile inclination on the distribution of displacements, stresses, axial forces, shear forces and bending moments in different piles in a group using a non-linear three-dimensional finite element technique.

Based on the above literature, numerical computations were carried out to study the influence of cyclic loading on the load deflection behaviour of laterally loaded pile groups, and the findings are reported in this paper.

Finite Element Formulation

The pile and soil are discretised into a number of 20 noded isoparametric continuum elements, The interface between pile and soil is modelled using 16 noded isoparametric surface elements, with zero thickness. These interface elements are useful in simulating the mechanics of stress transfer along the interface.

Continuum Element

Relation between strains and nodal displacements is expressed as,

$$\{\varepsilon\}_e = [B]\{\delta\}_e \tag{1}$$

where $\{\varepsilon\}_e$ = strain vector,

$\{\delta\}_e$ = vector consisting of nodal displacements, and

$[B]$ = strain-displacement transformation matrix,

The stress-strain relation is given by,

$$\{\sigma\}_e = [D]\{\varepsilon\}_e \tag{2}$$

where $\{\sigma\}_e$ = stress vector and

$[D]$ = constitutive relation matrix.

The stiffness matrix of an element is given as

$$K]_e = \int_v [B]^T [D][B]dv \tag{3}$$

Interface Element

The relative displacements (strains) between the surfaces of soil and structure induce stresses in the interface element. These relative displacements are given as,

$$\{\varepsilon\} = [B]_f\{\delta\}_e \tag{4}$$

where $[B]_f$ represents the strain-displacement transformation matrix.

The element stiffness is obtained by the usual expression,

$$[K]_e = \int_s [B]_f^T [D][B]_f \, ds \tag{5}$$

where $[D]$ is the constitutive relation matrix for the interface.

Equivalent Nodal Force Vector for Uniformly Distributed Shear

The lateral force, H, acting on the pile cap, is considered as uniformly distributed shear force over the cross-section of the pile. The intensity of this uniformly distributed force is, $q = H/A$, where A is the cross-sectional area. Equivalent nodal force vector, $\{Q\}_e$, is then expressed as,

$$\{Q\}_e = \int_A q[N]^T dA \tag{6}$$

where $[N]$ represents matrix of shape functions.

Constitutive Model

In this study, the pile is assumed to be linearly elastic. Nonlinearity of the soil medium is represented by a bilinear model, in which, the yield surface is described by von-Mises yield criterion, in terms of yield function, F, as

$$F = J_{D2} - \sigma_y = 0 \tag{7}$$

where σ_y indicates an experimentally determined yield stress and J_{D2} is the second deviatoric stress invariant.

In terms of the stresses, von-Mises criterion is

$$F = \left[\frac{1}{2}(\sigma_x - \sigma_y)^2 + \frac{1}{2}(\sigma_y - \sigma_z)^2 + \frac{1}{2}(\sigma_z - \sigma_x)^2 + 3\tau_{xy}^2 + 3\tau_{yz}^2 + 3\tau_{zx}^2 \right]^{1/2} - \sigma_y = 0 \tag{8}$$

It is also expressed as,

$$F = \sigma' - \sigma_y = 0 \tag{9}$$

where σ' is the effective or equivalent stress.

Effective or equivalent strain, ε', corresponding to the equivalent stress σ', is given in terms of co-ordinate strains as,

$$F = \frac{1}{\sqrt{2}(1+\nu_s)}\left[\begin{array}{c}(\varepsilon_x-\varepsilon_y)^2+(\varepsilon_y-\varepsilon_z)^2+(\varepsilon_z-\varepsilon_x)^2 \\ +\frac{3}{2}(\gamma_{xy}^2+\gamma_{yz}^2+\gamma_{zx}^2)\end{array}\right]^{1/2} = 0 \qquad (10)$$

From Eqns. 9 and 10, von-Mises yield criterion can be written in terms of effective strain, ε', and yield strain, ε_y, as

$$F = E(\varepsilon'-\varepsilon_y) = 0 \qquad (11)$$

Unloading is assumed to take place in a purely elastic manner, with elastic components of strain being independent of plastic deformation.

Nonlinearity of interface is also modelled using bilinear relationship. The shear stress components in $\{\sigma\}_e$ vector, and shear strain components in $\{\varepsilon\}_e$ vector are added vectorially to get the resultant shear stress, σ' and resultant shear strain, ε'. The interface is considered to yield when the resultant shear stress exceeds the yield value of shear stress for the interface.

Material Properties

Pile is assumed to be linearly elastic, defined by Young's modulus, E, and Poisson's ratio, ν. The soil behaviour is treated as bilinear with moduli, E_1 and E_2, before and after yielding, respectively, with Poisson's ratio ν_s, Interface behaviour is also modelled as bilinear, with shear stiffnesses, k_{s1} and k_{s2}, before and after yielding, respectively. The normal stiffness, k_n, of the interface is assumed to be constant.

Effect of Cyclic Loading on Soil and Interface Behaviour (Poulos, 1982)

For a clay loaded under undrained conditions, cyclic loading may have two important effects. It may lead to reduction in soil modulus and undrained shear strength, which, in turn lead to reduction in yield stress, σ_y, yield shear stress, τ_y, of interface and interface shear stiffness, k_s, These effects which are associated with the generation of excess pore pressure during the cyclic loading process, should be taken into account while analysing the response of a pile to cyclic loading. The most satisfactory means of performing this analysis would be to consider each cycle of loading separately, with soil parameters being progressively adjusted after each cycle.

A convenient means of defining the effects of cyclic loading on soil parameters is in terms of degradation factors, which express the ratio of the parameter for cyclic loading to the value of parameter for a single static load application. The degradation factor, D_e, for soil modulus and D_p, for yield pressure are therefore defined as,

$$D_e = \frac{E_c}{E_s} = \frac{k_{sc}}{k_{ss}} \quad \text{and} \quad D_p = \frac{\sigma_{yc}}{\sigma_{ys}} = \frac{\tau_{yc}}{\tau_{ys}} \tag{12}$$

in which,

E_s = soil moduli for static loading,

E_c = soil moduli for cyclic loading,

k_{ss} = interface shear stiffness for static loading,

k_{sc} = interface shear stiffness for cyclic loading,

σ_{ys} = yield pressures for static loading

σ_{yc} = yield pressures for cyclic loading and

τ_{ys} = yield shear stresses at interface for static loading

τ_{yc} = yield shear stresses at interface for cyclic loading.

From the relatively small amount of data available, the degradation factors for a saturated clay under undrained conditions appear to be related to the cyclic strain. Based on the data summarised by Idriss et al. (1978), for San Francisco Bay mud, the degradation factors D_p and D_e are expressed as follows,

$$\alpha = D_e = D_p = N^{-t} \tag{13}$$

in which

α represents degradation factor,

N represents no of cycles, and

t represents degradation parameter depending on cyclic normal strain.

Figure 1 shows a plot of degradation parameter, t, versus cyclic strain ratio, $\varepsilon_c/\varepsilon_{cr}$, derived from the data, presented by Idriss et al. (1978). ε_c is the cyclic strain and ε_{cr}, is a reference value of cyclic strain. The cyclic degradation behaviour of different soil types can be modified by altering the value of cyclic reference strain, ε_{cr}. Smaller the value of ε_{cr}, smaller is the cyclic strain necessary to produce a given amount of degradation, i.e. more susceptible is the soil to cyclic degradation.

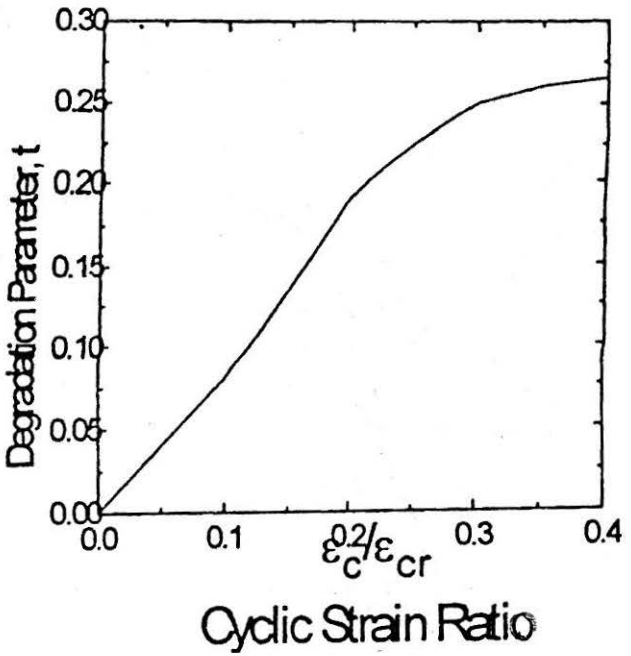

FIGURE 1 : Degradation Parameter, t

Iterative Procedure

The effect of cyclic loading is incorporated by allowing the reductions of soil modulus and yield stress, with increasing cyclic strain, at every cycle. The hysteretic behaviour in a typical stress-strain curve under the action of loading, unloading and subsequent reloading is shown in Figs. 2 and 3. This type of modelling of the non-linear behaviour of soil not only helps in tracing the loading and unloading paths, but also estimates the cyclic response of pile in a more realistic manner. The development of the procedure is based on the evaluation of stresses and strains pertaining to a constant stiffness, for various iterative steps at every cycle. The difference between the computed stress and the stress that is consistent with the computed strain is used to compute the load vector for the next iteration. Because constant stiffness is employed in all the iterations, this procedure offers a unique advantage for analysing a non-linear problem. Various iterative steps involved in the analysis for loading and unloading of each cycle are given below.

Loading

1. For the given loading, elastic analysis based on initial tangent modulus of bilinear relationship is performed to obtain nodal displacements.

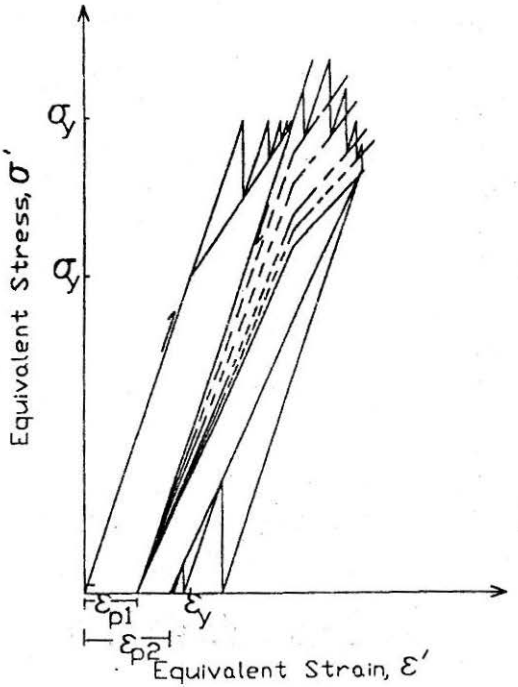

FIGURE 1 : Representation of Analysis for One-way Cyclic Loading

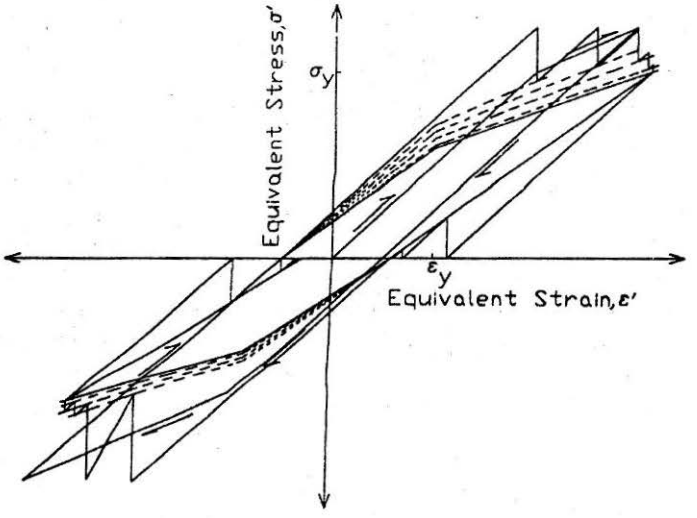

FIGURE 3 : Representation of Analysis for Two-way Cyclic Loading

2. Stresses and strains in the soil and interface elements are obtained from,

$$\{\varepsilon\}_e = [B]\{\delta\}_e \quad \text{and} \quad \{\sigma\}_e = [D]\{\varepsilon\}_e \tag{14}$$

The equivalent strain, ε', at any point (x, y, z) in the soil continuum is given by

$$\varepsilon' = \frac{1}{\sqrt{2}(1+\nu_s)}\left[\begin{matrix}(\varepsilon_x-\varepsilon_y)^2+(\varepsilon_y-\varepsilon_z)^2+(\varepsilon_z-\varepsilon_x)^2 \\ +\frac{3}{2}(\gamma_{xy}^2+\gamma_{yz}^2+\gamma_{zx}^2)\end{matrix}\right]^{1/2} \tag{15}$$

For interface elements, the shear strain components in $\{\varepsilon\}_e$ vector, are added vectorially to get resultant shear strain ε'. From Fig. 1, degradation parameter, t, is determined for the strain ratio $\varepsilon'/\varepsilon_{cr}$ (Poulos, 1982). The degradation factor, α, is computed using the following relation,

$$\alpha = N^{-t} \tag{16}$$

3. Extra stress vector, $\{\Delta\sigma\}_e$, which is the difference between the computed stress and the stress consistent with the computed strain, ε', is evaluated by using the expressions given in the Appendix.

4. The corresponding nodal force vector, $\{\Delta Q\}_e$, for the next iteration is given as follows,

$$\{\Delta Q\}_e = \int_v [B]^T\{\Delta\sigma\}dv \tag{17}$$

and for interface element

$$\{\Delta Q\}_e = \int_s [B]_f^T\{\Delta\sigma\}ds \tag{18}$$

5. Finite element analysis for the assembled correcting force vector is performed, with no change in the stiffness matrix.

6. This analysis gives increments in the nodal displacements, $\{\Delta\delta\}$. The

revised nodal displacements, $\{\delta\}$, are obtained from the following expression,

$$\{\delta\} = \{\delta\} + \{\Delta\delta\} \tag{19}$$

7. Procedure is repeated until satisfactory convergence is obtained.

Unloading

Same iterative procedure is used for unloading. Final set of values of degradation factors are used in unloading, and as the stresses in the soil are reduced in the process, its behaviour is considered linear. Details are given in the Appendix.

Problem Description

All piles considered in the analysis are square steel piles. Square piles are more convenient for mesh generation, however circular piles can also be considered as square piles with equivalent cross sectional area and flexural rigidity. Trend shown by the results would not be different. Material properties of pile, soil and interface media are described in Table 1. A value of 0.02, for reference cyclic stain, ε_{cr}, as suggested by Poulos (1982), is used in the analysis. When the direction of loading is parallel to the line joining piles, it is referred as a series arrangement. On the other hand, if the lateral loading is acting in a direction perpendicular to the line joining piles, it is a parallel arrangement (Fig. 4). Analysis is performed for 100 cycles of

Table 1
Material Properties of Pile, Soil and Interface Media

Pile	Soil	Interface
$E_p = 2.0 \times 10^8$ kN/m^2	$E_1 = 4267$ kN/m^2, and $E_2 = 0$	$k_{s1} = 1000$ kN/m^3 $k_n = 1.0 \times 10^6$ kN/m^3 $k_{s2} = 0$
$\nu = 0.15$	$\nu_s = 0.45$	
Width D = 1 m	$\varepsilon_y = 0.02$	$\varepsilon_y = 0.02$
Length L = 25 m Pile cap thickness = 0.15 m	$\varepsilon_{cr} = 0.02$	$\varepsilon_{cr} = 0.02$

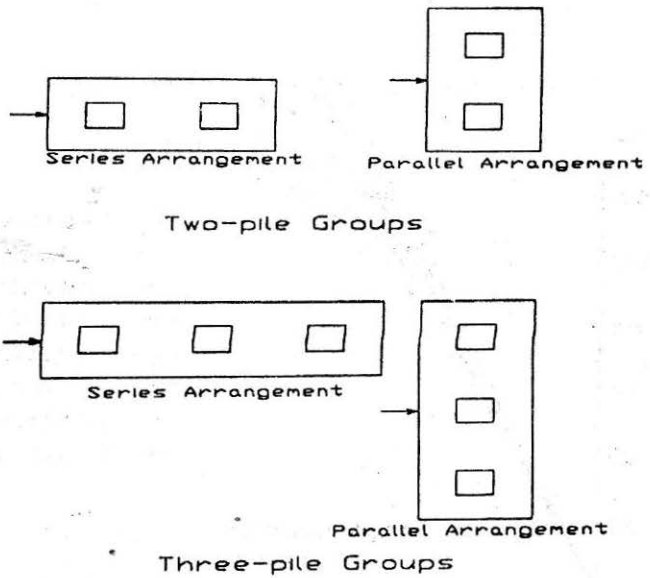

FIGURE 4 : Arrangement of Piles in Groups

one-way and two-way cyclic loading. In one-way cyclic loading, load increases from zero to positive maximum value and reduces to zero, whereas, in two-way cyclic loading, load path is zero-maximum positive value-zero-maximum negative value-zero. Following cases are considered in the analysis:

1. Two-pile group in series arrangement with spacings 2.5D, 3D, 4D and 5D.
2. Two-pile group in parallel arrangement with spacings 2.5D, 3D, 4D and 5D.
3. Three-pile group in series arrangement with spacings 2.5D, 3D, 4D and 5D.
4. Three-pile group in series arrangement with spacings 2.5D, 3D, 4D and 5D.
5. Single pile

Results

Maximum applied loads for two-pile and three-pile groups are 1500 kN and 2000 kN respectively. But in some cases, convergence is not achieved due to large incremental displacements, before reaching 100 cycles of load

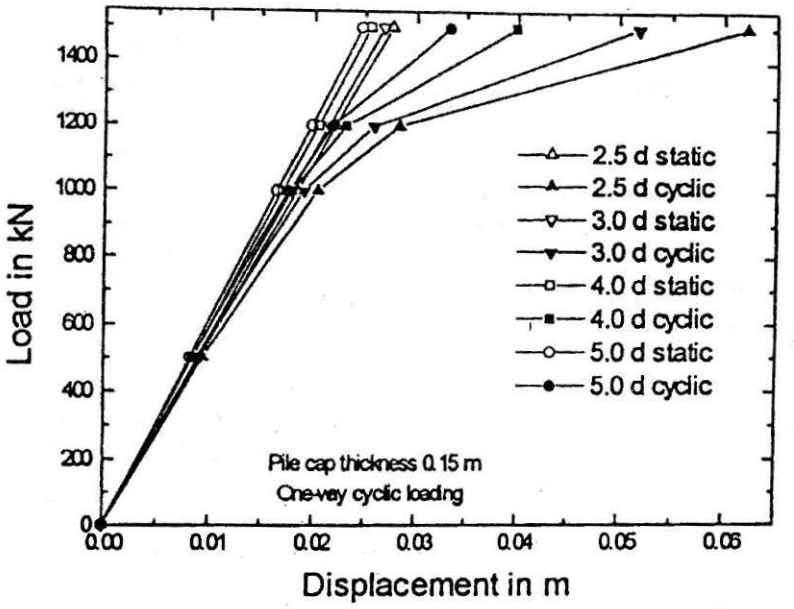

Fig. 5(a)

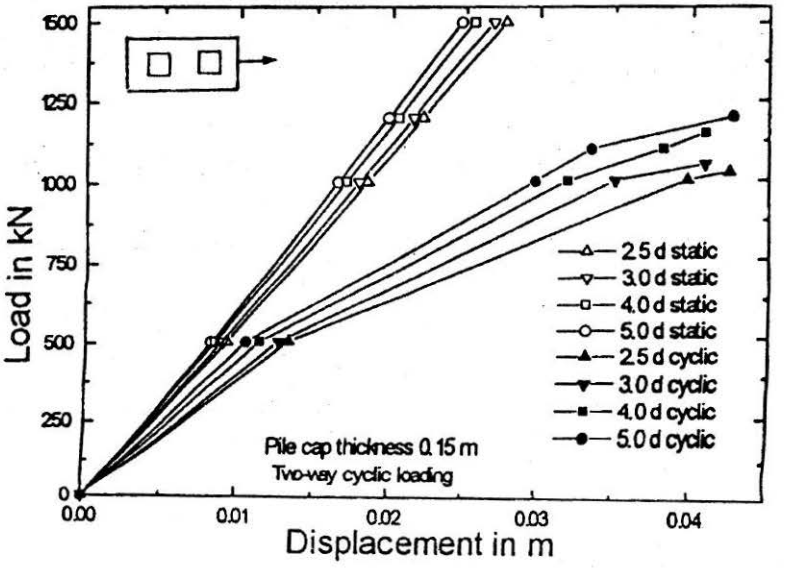

FIGURE 5 : Load–Deflection Curve for Two-Pile Group in Series

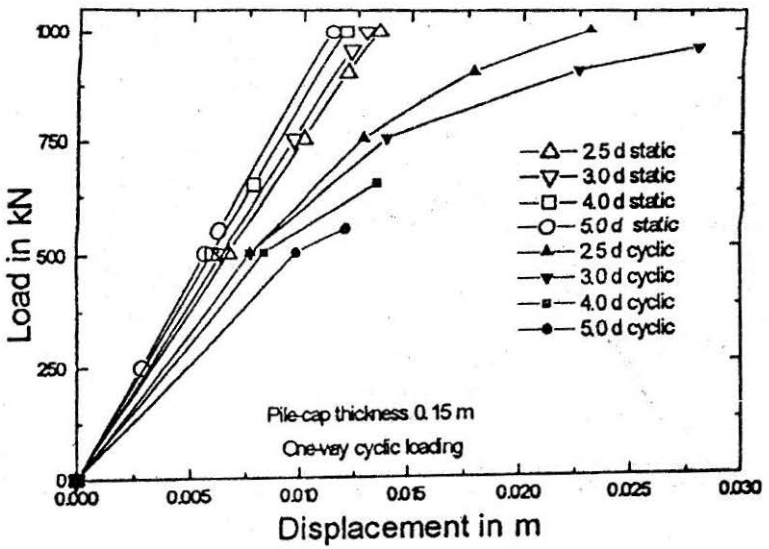

Fig. 6(a)

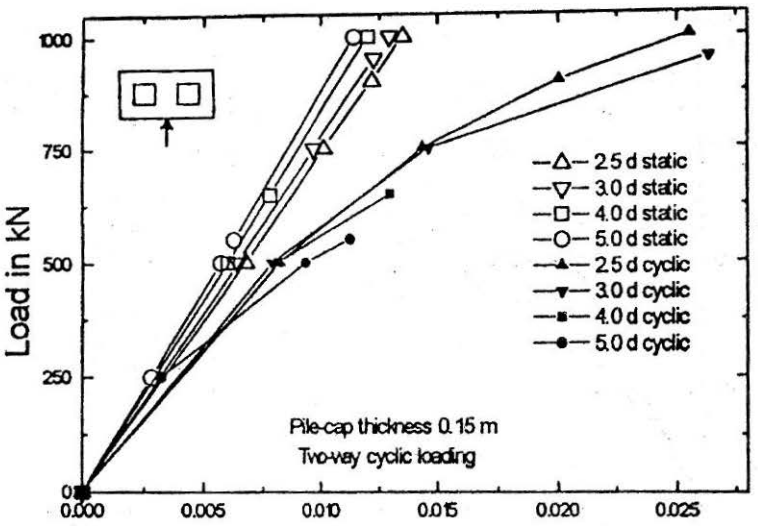

FIGURE 6 : Load-Deflection Curve for Two-Pile Group in Parallel

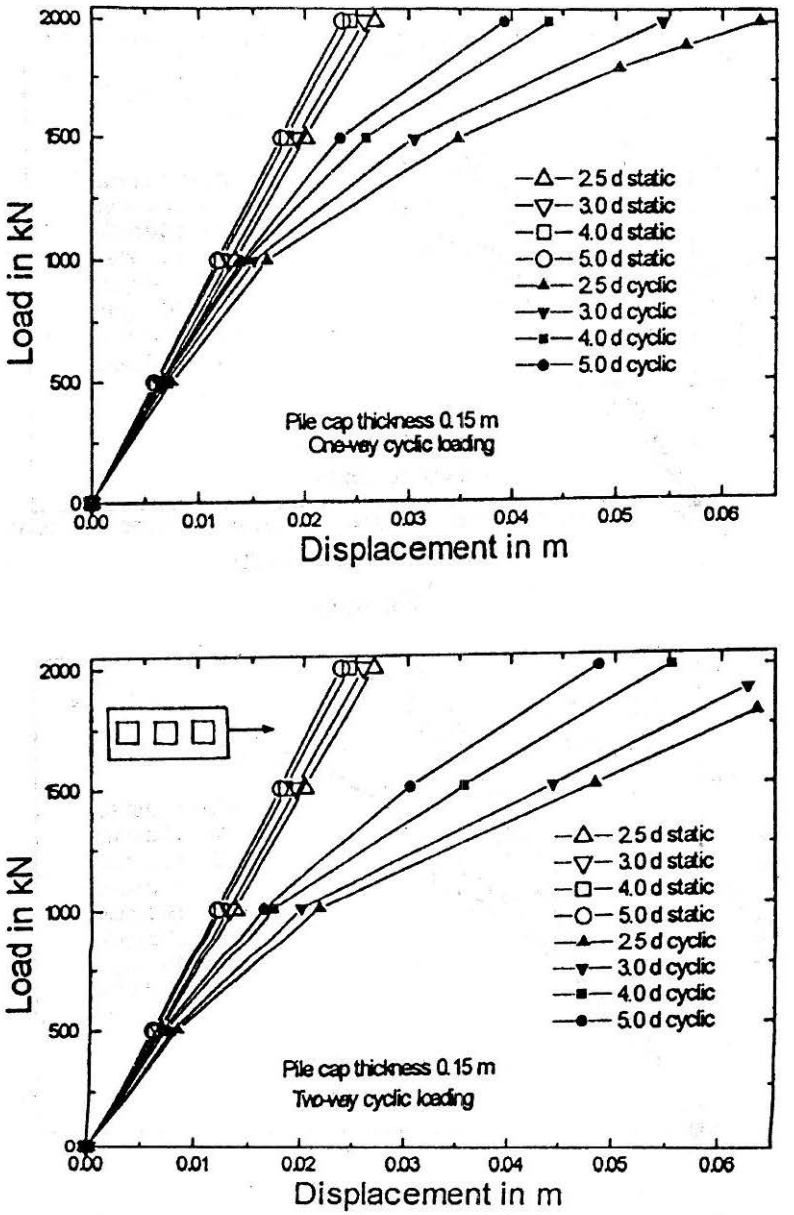

FIGURE 7 : Load–Deflection Curve for Three-Pile Group in Series

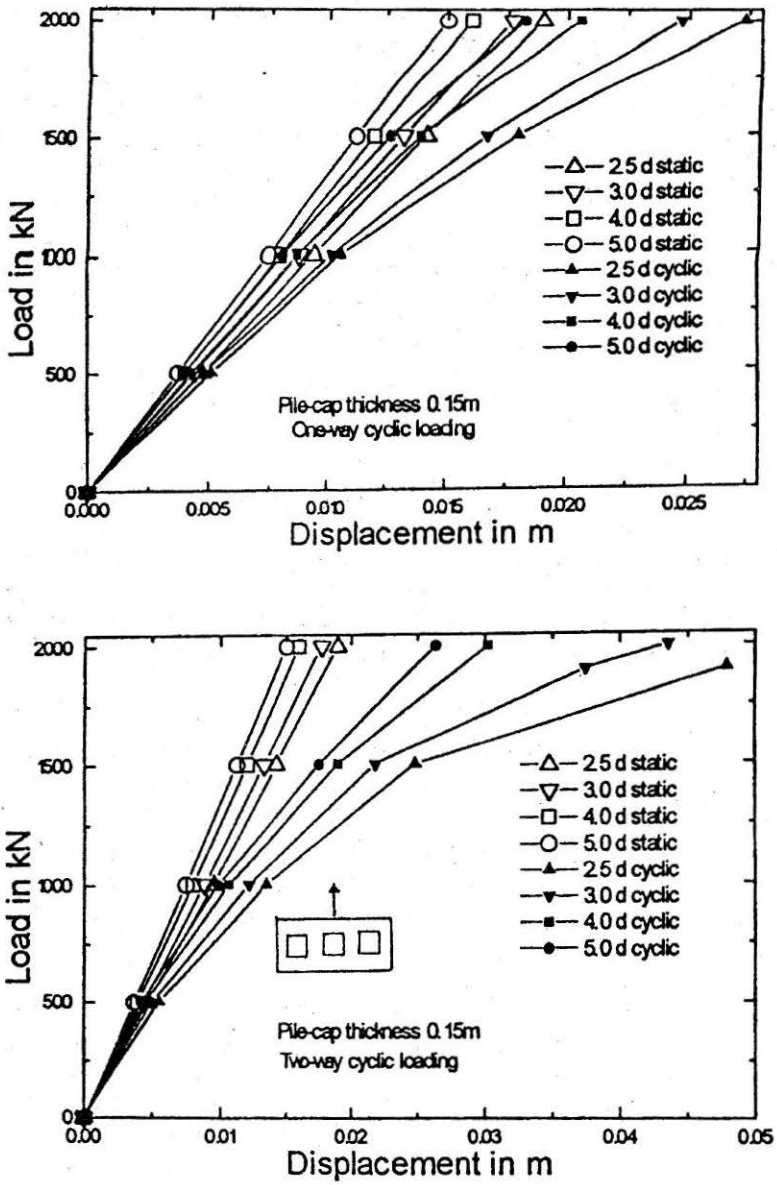

FIGURE 8 : Load–Deflection Curve for Three-Pile Group in Parallel

application. In that case, the maximum load upto which analysis is performed for 100 cycles, is considered as ultimate load.

Figures 5 to 8 describe the effect of cyclic loading, and pile spacing on load-deflection behaviour, for different pile configurations. There is a substantial increase in the pile top displacements after 100 cycles. From Fig. 5 it is observed that the capacity of pile group increases with increase in spacing for both static and cyclic loading. This may be due to the overlapping stressed zones of individual piles at closer spacing.

Load–deflection curves for two-pile group with parallel arrangement (Fig. 6) show different behaviour for cyclic loading. Considerable reduction in capacity of pile group is observed with increase in spacing, under cyclic loading. This phenomenon can be explained as follows:

As spacing between piles increases, flexibility of pile and pile cap system increases. On the contrary, larger area of soil foundation is available for development of passive resistance with increase in spacing, as a result of which, total pile-soil-pile system offers more resistance to static loading. Increase in total stiffness in case of static loading is as a result of increase in soil stiffness, though structural stiffness (pile and pile cap) is decreasing, whereas under cyclic loading, soil stiffness is considerably reduced due to degradation. Hence under cyclic loading, total stiffness of pile–soil system reduces with increase in spacing between the piles.

Load–deflection curve for three-pile group in series arrangement (Fig. 7) and parallel arrangement (Fig. 8) show similar behaviour as two-pile group in series arrangement. It can be seen that effect of cyclic loading, increases with decreasing spacing. Tables 2 and 3 report the maximum percentage increase in the pile top displacements, and maximum moment, for one-way and two-way cyclic loading, respectively. Increase in maximum moment is 29 to 36%. There is not much difference in moments for one-way and two-way cyclic loading.

Figures 9 and 10 compare load-deflection behaviour of two-pile and three-pile groups in series and parallel arrangement for static and cyclic loading. It is observed that piles in parallel arrangement offer more resistance compared to the piles in series arrangement. This can be attributed to the larger area available for development of passive resistance.

Typical moment distribution along depth for three-pile group is shown in Fig. 11. The effect is more pronounced in lower half of pile. Figure 12 shows load-deflection curve for single pile. Yielding of pile takes place at 375 kN for one-way cyclic loading, and at 400 kN for two-way cyclic loading.

Table 2
Maximum Percentage Increase in Displacement and Moment for One-way Cyclic Loading for Different Pile Configurations

Configuration	Spacing 2.5 D			Spacing 3.0 D			Spacing 4.0 D			Spacing 5.0 D		
	Load	Disp.	Moment	Load	Disp.	Moment	Load	Disp.	Moment	Load	Disp.	Moment
Two-pile series	1500 kN	124.74	29.54	1500 kN	93.1	30.214	1500 kN	56.143	30.818	1500 kN	35.03	30.544
Two-pile Parallel	1000 kN	70.53	29.26	950 kN	127.74	28.19	650 kN	73.19	13.86	550 kN	93.89	11.93
Three-pile series	2000 kN	137.25	30.67	2000 kN	111.64	30.82	2000 kN	79.44	30.03	2000 kN	66.89	28.19
Three-pile Parallel	2000 kN	44.09	35.59	2000 kN	39.54	35.58	2000 kN	28.23	33.09	2000 kN	21.58	31.43

Table 3
Maximum Percentage Increase in Displacement and Moment for Two-way Cyclic Loading for Different Pile Configurations

Configuration	Spacing 2.5 D			Spacing 3.0 D			Spacing 4.0 D			Spacing 5.0 D		
	Load	Disp.	Moment	Load	Disp.	Moment	Load	Disp.	Moment	Load	Disp.	Moment
Two-pile series	1025 kN	124.57	29.77	1050 kN	117.64	30.25	1150 kN	127.53	32.42	1200 kN	115.80	30.422
Two-pile Parallel	1000 kN	88.96	29.22	950 kN	114.98	28.09	650 kN	66.39	13.82	550 kN	79.79	11.79
Three-pile series	1800 kN	162.96	31,86	1900 kN	156.02	32.60	2000 kN	127.20	31.56	2000 kN	105.81	29.36
Three-pile Parallel	1900 kN	166.09	36.43	2000 kN	146.12	36.20	2000 kN	88.67	33.68	2000 kN	75.96	31.28

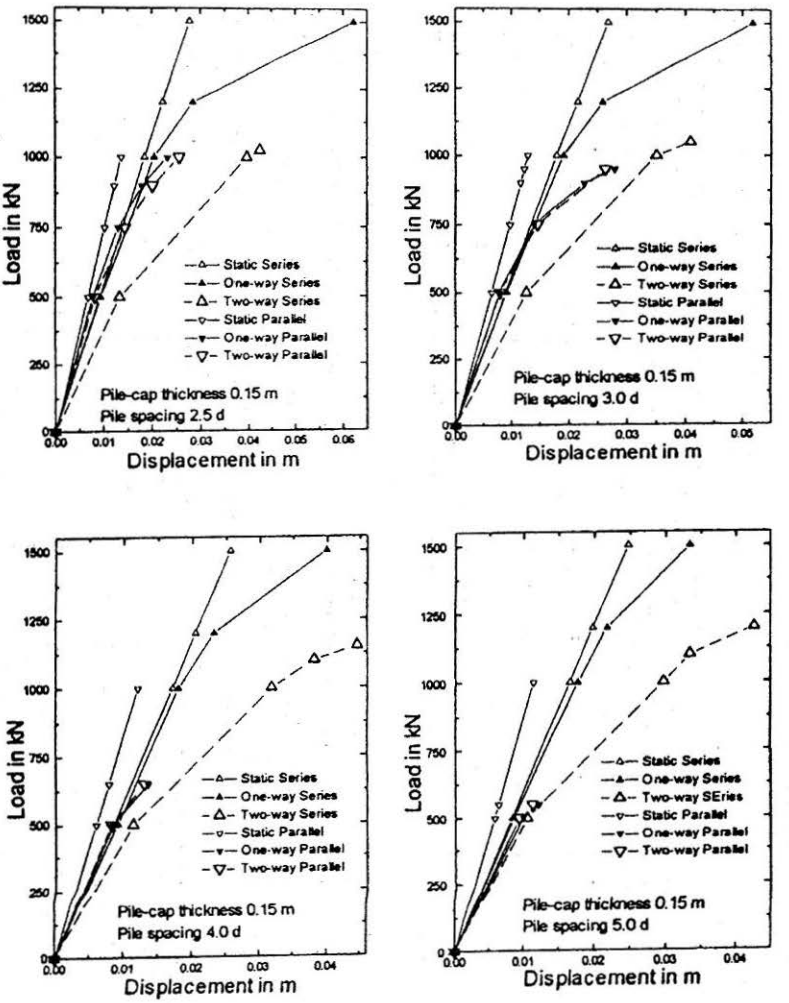

FIGURE 9 : Comparison of Load-Deflection Behaviour of Two-Pile Groups

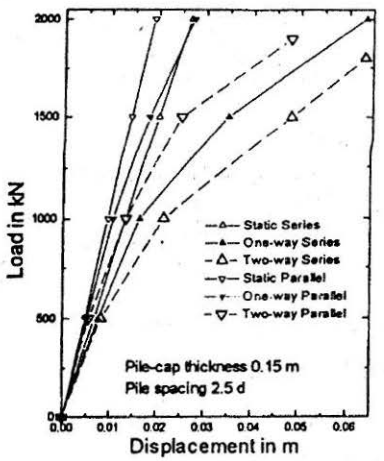

Fig. 10(a)

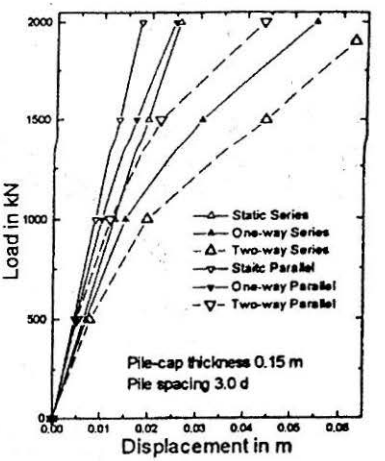

Fig. 10(b)

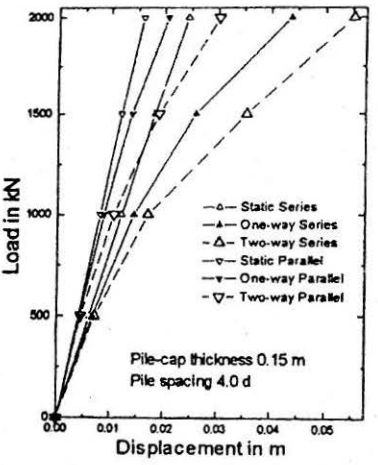

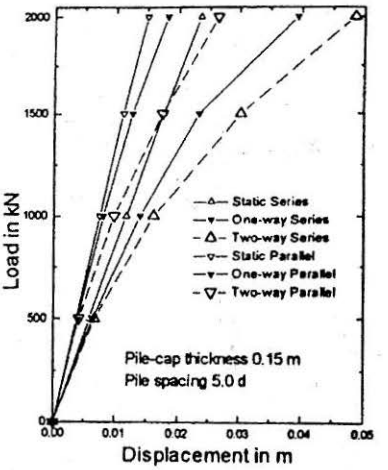

FIGURE 10 : Comparison of Load-Deflection Behaviour of Three-Pile Groups

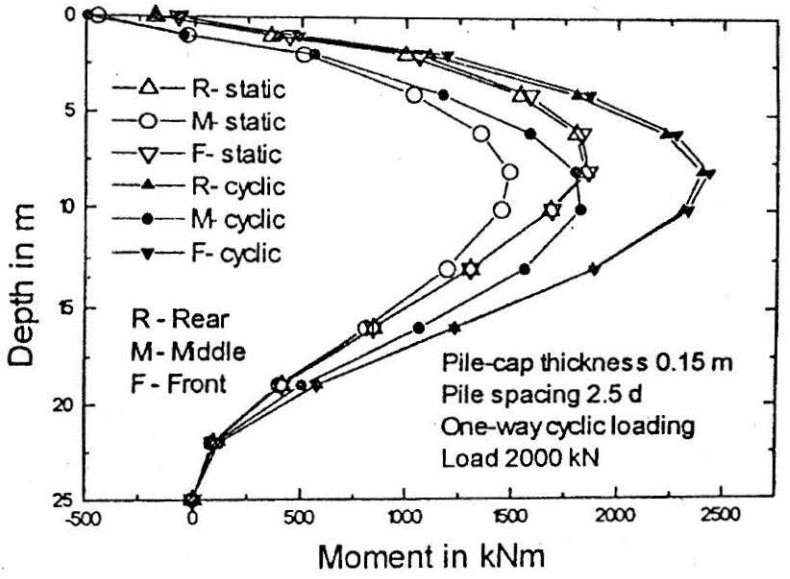

FIGURE 11 : Distribution of Moment along Depth (Three-Pile Group Series)

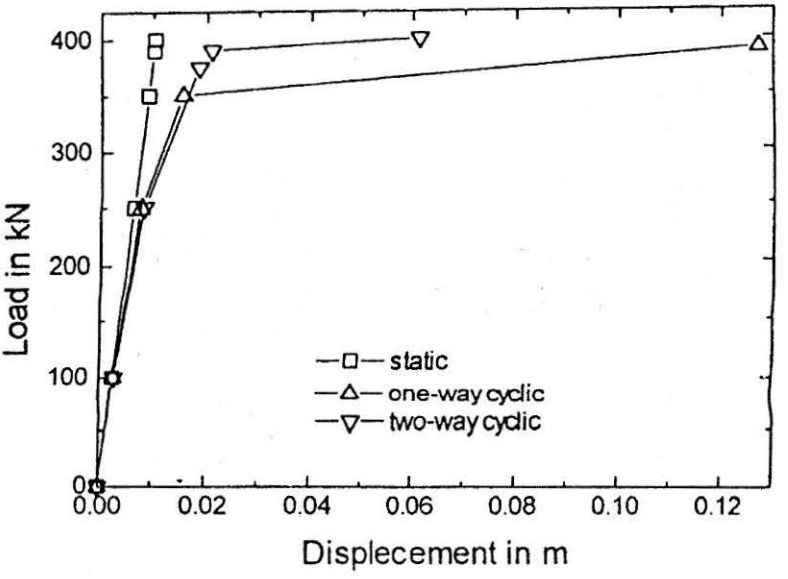

FIGURE 12 : Load Deflection Curve for Single Pile

Table 4
Pile Group Efficiencies for Cyclic Loading

Pile Configuration	Spacing 2.5 D	Spacing 3 D	Spacing 4 D	Spacing 5 D
Two-pile series	1.28	1.31	1.44	1.5
Two-pile parallel	1.25	1.19	0.81	0.69
Three-pile series	1.5	1.58	> 1.67	> 1.67
Three-pile parallel	1.58	> 1.67	> 1.67	> 1.67

Group efficiency for cyclic loading is estimated using the following expression,

$$\text{Group Efficiency} = \frac{\text{Ultimate Load for Pile Group}}{(\text{No. of Piles}) \times (\text{Ultimate Load for Single Pile})}$$

Table 4 shows the group efficiencies for different spacings, and pile configurations. It is seen that group efficiency generally increases with increase in spacing.

Conclusions

The analysis presented considers two important factors, degradation of soil modulus and yield stress, and accumulation of permanent displacements. It reproduces the observed characteristics of pile behaviour under cyclic loading reasonably well, namely, an increase in deflection and moment with increasing number of cycles and increasing load level, and a decrease in ultimate lateral load capacity. Apart from the usual data required for a static analysis, the only additional data required for a cyclic analysis are the variation of degradation parameter, t, with cyclic strain.

Following conclusions are drawn from the present study :

1. Effect of two-way cyclic loading is more as compared to one-way cyclic loading, when displacements are considered, while, one-way cyclic loading and two-way cyclic loading have the same effect on moment distribution in the pile.

2. There is significant increase in the pile top displacement, whereas, maximum increase in maximum moment is only 29 to 36 %.

3. Ultimate lateral load capacity of pile group for cyclic loading generally increases with increase in spacing.

4. Piles in parallel arrangement offer more resistance compared to the piles in series arrangement

5. More increase in moment occurs in the lower half of the pile under cyclic loading condition.

References

BANERJEE, P.K. and DRISCOLL, R.M. (1976) : "Three-Dimensional Analysis of Vertical Pile Groups", *Proc. of Second International Conference on Numerical Methods in Geomechanics*, Blacksburg, Vol.1, pp.438-450.

DESAI, C.S., KUPPUSAMY, T. and ALAMEDDINE, A.R. (1981) : "Pile Cap Pile Group Soil Interaction", *Journal of Struct. Engg. Div.*, ASCE, 107, ST5.

HRENNIKOFF, A. (1949) : "Analysis of Pile Foundation with Batter Piles", *Proc.*, ASCE.

IDRISS, L.M., DOBRY, R. and SINGH, R.D. : "Nonlinear Behaviour of Soft Clays During Cyclic Loading", *Journal of Geotechnical Engg Div.*, ASCE. Vol.104, GT12, pp.1427-1447.

KIM, J.B. and BRUNGRABER, R.J. (1976) : "Full Scale Lateral Load Tests of Pile Groups", *Journal of Geotechnical Engg.*, ASCE, Vol.108, Jan., pp.87-105.

MUQTADIR, A. and DESAI, C.S. (1986) : "Three-Dimensional Analysis of a Pile-group Foundation", *International Journal for Numerical Methods in Geomechanics*, Vol.10, pp.41-58.

POULOS, H.G. (1982) : "Single Pile Response to Cyclic Lateral Loads", *Journal of Geotechnical Engg.*, Vol.108, GT3, pp.711-731.

REESE, L.C. and O'NEILL, M.W. (1970) : "Generalised Analysis of Pile Foundations", *Journal of Soil Mech. and Found. Div.*, ASCE, 96, SM1.

ZAMAN, M.M., NAJAR, Y.M. and MUQTADIR, A. (1993) : "Effects of Cap Thickness and Pile Inclination on the Response of a Pile Group by a Three-Dimensional Non-linear Finite Element Analysis", *Computers and Geotechnics*, 15, pp.65-86.

Notations

A = Area of pile or pile cap

α = Degradation factor

$[B]$ = Strain-displacement transformation matrix

$[B]_f$ = Strain-displacement transformation matrix for interface element

D = Width of square pile

D_e = Degradation factor for soil modulus

D_p = Degradation factor for yield pressure

$[D]$ = Constitutive matrix

$\{\delta\}$ = Nodal displacement vector

$\{\Delta\sigma\}_e$ = Extra stress vector

E_p = Young's modulus of 0000000pile

E_1 = Soil modulus before yielding

E_2 = Soil modulus after yielding

ε' = Equivalent strain

$\{\varepsilon\}_e$ = Strain vector

ε_{cr} = Reference cyclic strain

ε_y = Yield strain

F = Yield function

H = Applied horizontal load

J_{D2} = Second deviatoric stress invariant

$[K]_e$ = Element stiffness matrix

k_n = Normal stiffness

k_{s1} = Shear stiffness before yielding

k_{s2} = Shear stiffness after yielding

L = Length of pile

ν = Poisson's ratio of pile

ν_s = Poisson's ratio of soil

N = Number of cycle

$[N]$ = Shape functions

$\{Q\}$ = Load vector

q	=	Uniformly distributed load
$\{\sigma\}_e$	=	Stress vector
σ'	=	Equivalent stress
σ_y	=	Yield stress
t	=	Degradation parameter
τ_y	=	Yield shear stress
u	=	Displacement in X direction
v	=	Displacement in Y direction
w	=	Displacement in Z direction
(x, y, j)	=	Global co-ordinates
(ξ, η, ζ)	=	Local co-ordinates

APPENDIX

Computation of Extra Stress Vector

Loading

The extra stress vector, $\{\Delta\sigma\}_e$, for first iteration is computed as follows

When ε' is less than yield strain ε_y

$$\{\Delta\sigma\}_e = (1-\alpha)[D]\{\varepsilon\}_e$$

and for interface element

$$\{\Delta\sigma\}_e = (1-\alpha)[D_m][D]\{\varepsilon\}_e \tag{A-1}$$

where

$$[D_m] = \begin{bmatrix} 1 & 0 & 0 \\ 0 & 1 & 0 \\ 0 & 0 & 0 \end{bmatrix} \tag{A-2}$$

When ε' is greater than yield strain

$$\{\Delta\sigma\}_e = \frac{E_1 - E_s}{E_1}[D]\{\varepsilon\}_e$$

and for interface element

$$\{\Delta\sigma\}_e = \frac{k_{s1} - k_{ss}}{k_{s1}}[D_m][D]\{\varepsilon\}_e \tag{A-3}$$

where, E_s and k_{ss} are the secant moduli, corresponding to strain ε' given by

$$E_s = \frac{\alpha E_1 \varepsilon_y + \alpha E_2(\varepsilon' - \varepsilon_y)}{\varepsilon'}$$

$$k_{ss} = \frac{\alpha k_{s1} \varepsilon_y + \alpha k_{s2}(\varepsilon' - \varepsilon_y)}{\varepsilon'} \tag{A-4}$$

The extra stress vector, $\{\Delta\sigma\}_e$, for next iteration is given by the following expressions

If ε' is less than yield strain ε_y, then

$$\{\Delta\sigma\}_e = (1-\alpha)[D]\{\Delta\varepsilon\}_e + (\alpha-\alpha')[D]\{\varepsilon\}_e$$

and for interface element

$$\{\Delta\sigma\}_e = (1-\alpha)[D_m][D]\{\Delta\varepsilon\}_e + (\alpha-\alpha')[D_m][D]\{\varepsilon\}_e \qquad \text{(A-5)}$$

If ε' is greater than yield strain, ε_y, and point is not yielded in previous iteration, then,

$$\{\Delta\sigma\}_e = \frac{E_1 - \frac{\Delta\bar{\sigma}}{\Delta\varepsilon'}}{E_1}[D]\{\Delta\varepsilon\}_e + (\alpha-\alpha')\frac{E_s}{E_1}[D]\{\varepsilon\}_e \qquad \text{(A-6)}$$

where

$$\Delta\bar{\sigma} = \alpha E_1(\varepsilon_y + \Delta\varepsilon' - \varepsilon) + \alpha E_2(\varepsilon' - \varepsilon_y) \qquad \text{(A-7)}$$

and for interface element

$$\{\Delta\sigma\}_e = \frac{k_{s1} - \frac{\Delta\bar{\tau}}{\Delta\varepsilon'}}{k_{s1}}[D_m][D]\{\Delta\varepsilon\}_e + (\alpha-\alpha')\frac{k_{ss}}{k_{s1}}[D_m][D]\{\varepsilon\}_e$$

..... (A-8)

where

$$\Delta\bar{\tau} = \alpha k_{s1}(\varepsilon_y + \Delta\varepsilon' - \varepsilon) + \alpha k_{s2}(\varepsilon' - \varepsilon_y) \qquad \text{(A-9)}$$

If ε' is greater than yield strain, ε_y and point is yielded in previous iteration, then

$$\{\Delta\sigma\}_e = \frac{E_1 - \alpha E_2}{E_1}[D]\{\Delta\varepsilon\}_e + (\alpha-\alpha')\frac{E_s}{E_1}[D]\{\varepsilon\}_e \qquad \text{(A-10)}$$

and for interface element

$$\{\Delta\sigma\}_e = \frac{k_{s1} - \alpha k_{s2}}{k_{s1}}[D_m][D]\{\Delta\varepsilon\}_e + (\alpha - \alpha')\frac{k_{ss}}{k_{s1}}[D_m][D]\{\varepsilon\}_e$$

..... (A-11)

Unloading

For unloading, the extra stress vector, $\{\Delta\sigma\}_e$, is calculated as

$$\{\Delta\sigma\}_e = (1-\alpha)[D]\{\Delta\varepsilon\}_e$$

and for interface element

$$\{\Delta\sigma\}_e = (1-\alpha)[D_m][D]\{\Delta\varepsilon\}_e \qquad \text{(A-12)}$$

Loading in opposite direction

The extra stress vector, $\{\Delta\sigma\}_e$, for first iteration is computed as follows:

Calculate the degradation parameter, α', for the equivalent strain, ε'. If α' is less than α, then set $\alpha = \alpha'$.

When ε' is less than yield strain, ε_y

$$\{\Delta\sigma\}_e = (1-\alpha)[D]\{\varepsilon\}_e$$

and for interface element,

$$\{\Delta\sigma\}_e = (1-\alpha)[D_m][D]\{\varepsilon\}_e \qquad \text{(A-13)}$$

When ε' is greater than yield strain, ε_y,

$$\{\Delta\sigma\}_e = \frac{E_1 - E_s}{E_1}[D]\{\varepsilon\}_e$$

and for interface element,

$$\{\Delta\sigma\}_e = \frac{k_{s1} - k_{ss}}{k_{s1}}[D_m][D]\{\varepsilon\}_e \qquad \text{(A-14)}$$

where, E_s and k_{ss} are the secant moduli, corresponding to strain, ε' and are given as

$$E_s = \frac{\alpha E_1 \varepsilon_y + \alpha E_2 (\varepsilon' - \varepsilon_y)}{\varepsilon'}$$

$$k_{ss} = \frac{\alpha k_{s1} \varepsilon_y + \alpha k_{s2} (\varepsilon' - \varepsilon_y)}{\varepsilon'} \qquad \text{(A-15)}$$

The extra stress vector, $\{\Delta\sigma\}_e$, for next iterations is given by the following expressions.

Set the degradation parameter in last iteration as α. Calculate new degradation parameter, α', for equivalent strain, ε'.

1. If α' greater than α, only α will be considered.

   a) If the point has failed in earlier iteration,

$$\{\Delta\sigma\}_e = \frac{E_1 - \alpha E_2}{E_1}[D]\{\Delta\varepsilon\}_e$$

   and for interface element,

$$\{\Delta\sigma\}_e = \frac{k_{s1} - \alpha k_{s2}}{k_{s1}}[D_m][D]\{\Delta\varepsilon\}_e \qquad \text{(A-16)}$$

   b) If the point has not failed in earlier iteration, then

      1) for ε' less than yield strain, ε_y,

$$\{\Delta\sigma\}_e = (1-\alpha)[D]\{\Delta\varepsilon\}_e$$

      and for interface element,

$$\{\Delta\sigma\}_e = (1-\alpha)[D_m][D]\{\varepsilon\}_e \qquad \text{(A-17)}$$

      2) for ε' greater than yield strain, ε_y,

$$\{\Delta\sigma\}_e = \frac{E_1 - E_s}{E_1}[D]\{\varepsilon\}_e$$

and for interface element,

$$\{\Delta\sigma\}_e = \frac{k_{sl} - k_{ss}}{k_{sl}}[D_m][D]\{\varepsilon\}_e \qquad \text{(A-18)}$$

where, E_s and k_{ss} are the secant moduli, corresponding to strain, ε' and are given as,

$$E_s = \frac{\alpha E_1 \varepsilon_y + \alpha E_2(\varepsilon' - \varepsilon_y)}{\varepsilon'}$$
$$k_{ss} = \frac{\alpha k_{s1} \varepsilon_y + \alpha k_{s2}(\varepsilon' - \varepsilon_y)}{\varepsilon'} \qquad \text{(A-19)}$$

2. If α' is less than α, both should be considered.

a) If the point has failed in earlier iteration,

$$\{\Delta\sigma\}_e = \frac{E_1 - \alpha E_2}{E_1}[D]\{\Delta\varepsilon\}_e + (\alpha - \alpha')\frac{E_s}{E_1}[D]\{\varepsilon\}_e \qquad \text{(A-20)}$$

and for interface element,

$$\{\Delta\sigma\}_e = \frac{k_{sl} - \alpha k_{s2}}{k_{sl}}[D_m][D]\{\Delta\varepsilon\}_e + (\alpha - \alpha')\frac{k_{ss}}{k_{sl}}[D_m][D]\{\varepsilon\}_e \qquad \text{(A-21)}$$

where

$$E_s = \frac{E_1 \varepsilon_y + E_2(\varepsilon' - \varepsilon_y)}{\varepsilon'}$$
$$k_{ss} = \frac{\alpha k_{s1} \varepsilon_y + \alpha k_{s2}(\varepsilon' - \varepsilon_y)}{\varepsilon'}$$

b) If the point has not failed in earlier iteration,

1) for ε' less than yield strain, ε_y,

$$\{\Delta\sigma\}_e = (1 - \alpha)[D]\{\Delta\varepsilon\}_e + (\alpha - \alpha')[D]\{\varepsilon\}_e$$

and for interface element,

$$\{\Delta\sigma\}_e = (1-\alpha)[D_m][D]\{\Delta\varepsilon\}_e + (\alpha-\alpha')[D_m][D]\{\varepsilon\}_e \quad \text{..... (A-22)}$$

2) for ε' greater than yield strain, ε_y,

$$\{\Delta\sigma\}_e = \frac{E_1 - \frac{\Delta\bar{\sigma}}{\Delta\varepsilon'}}{E_1}[D]\{\Delta\varepsilon\}_e + (\alpha-\alpha')\frac{E_s}{E_1}[D]\{\varepsilon\}_e \quad \text{..... (A-23)}$$

where

$$\Delta\bar{\sigma} = \alpha E_1(\varepsilon_y + \Delta\varepsilon' - \varepsilon) + \alpha E_2(\varepsilon' - \varepsilon_y)$$

$$E_s = \frac{E_1\varepsilon_y + E_2(\varepsilon' - \varepsilon_y)}{\varepsilon'} \quad \text{(A-24)}$$

for interface element,

$$\{\Delta\sigma\}_e = \frac{k_{s1} - \frac{\Delta\bar{\tau}}{\Delta\varepsilon'}}{k_{s1}}[D_m][D]\{\Delta\varepsilon\}_e + (\alpha-\alpha')\frac{k_{ss}}{k_{s1}}[D_m][D]\{\varepsilon\}_e \quad \text{(A-25)}$$

where

$$\Delta\bar{\tau} = \alpha k_{s1}(\varepsilon_y + \Delta\varepsilon' - \varepsilon) + \alpha k_{s2}(\varepsilon' - \varepsilon_y)$$

$$k_{ss} = \frac{\alpha k_{s1}\varepsilon_y + \alpha k_{s2}(\varepsilon' - \varepsilon_y)}{\varepsilon'} \quad \text{(A-26)}$$